

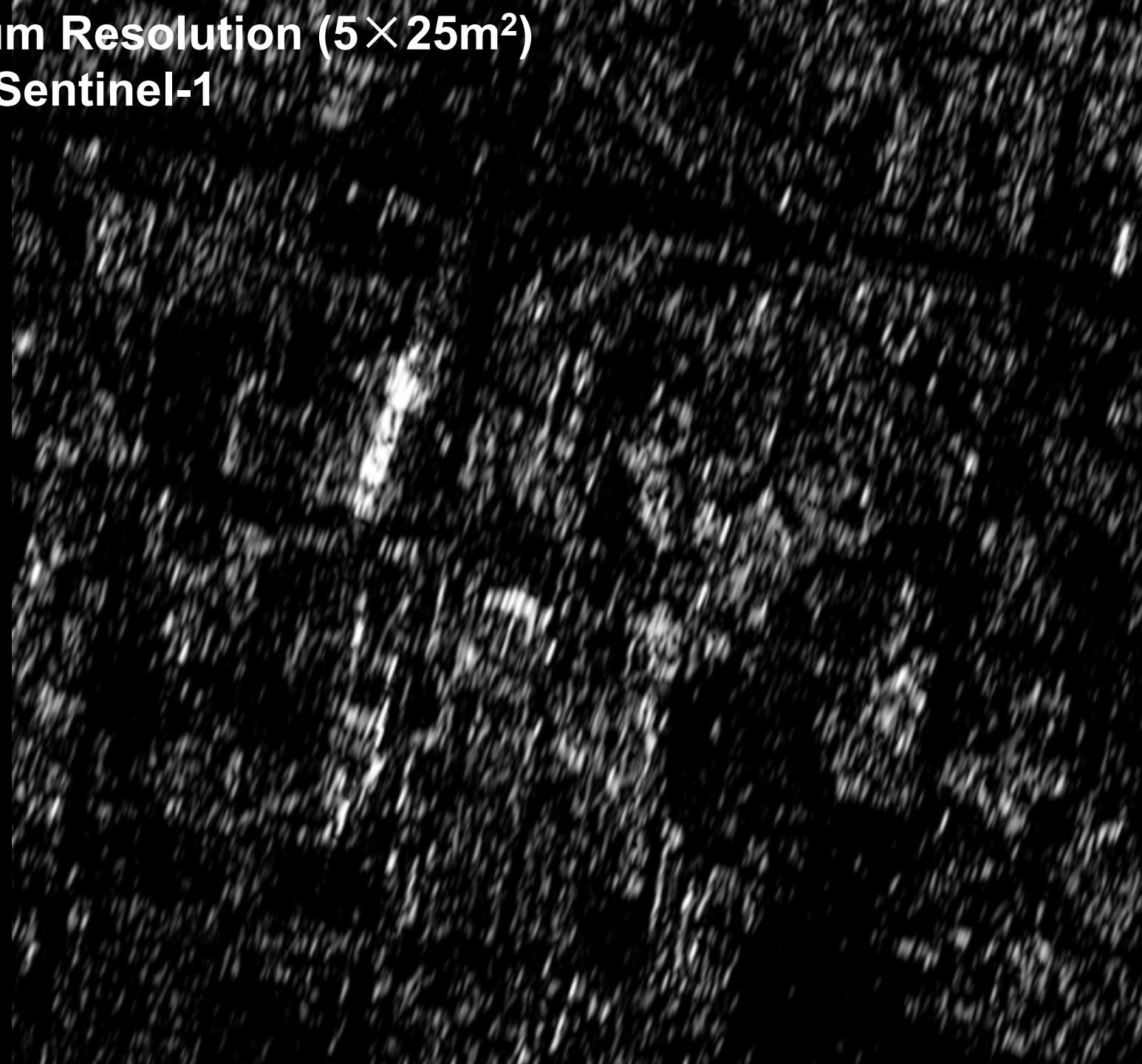
Multi-temporal High-Resolution SAR for Geometric Measurements and for Ground Deformation Monitoring

Michael Eineder & SAR teams
Remote Sensing Technology Institute, DLR &
Technische Universität München

Knowledge for Tomorrow



**Medium Resolution ($5 \times 25\text{m}^2$)
ERS, Sentinel-1**



**Very High Resolution ($1.1 \times 0.6 \text{ m}^2$)
TerraSAR-X**

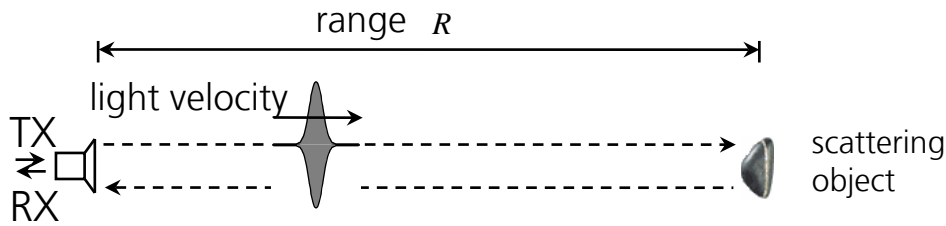


Outline

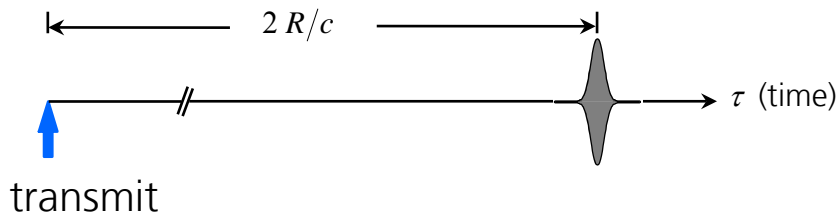
- Short tutorial *Accuracy of SAR geometry*
 - Methods for error reduction
 - Range & azimuth measurements
 - Exploitation of accurate geometry
- Some recent examples from TerraSAR-X and TanDEM-X



“Range” Measurements with SAR: How Accurate?

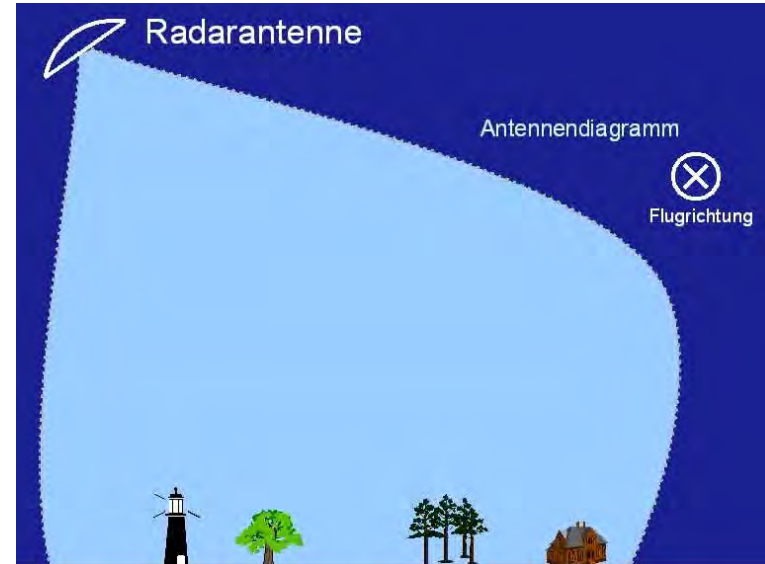


received echo:



$$R = \frac{\tau c'}{2}$$

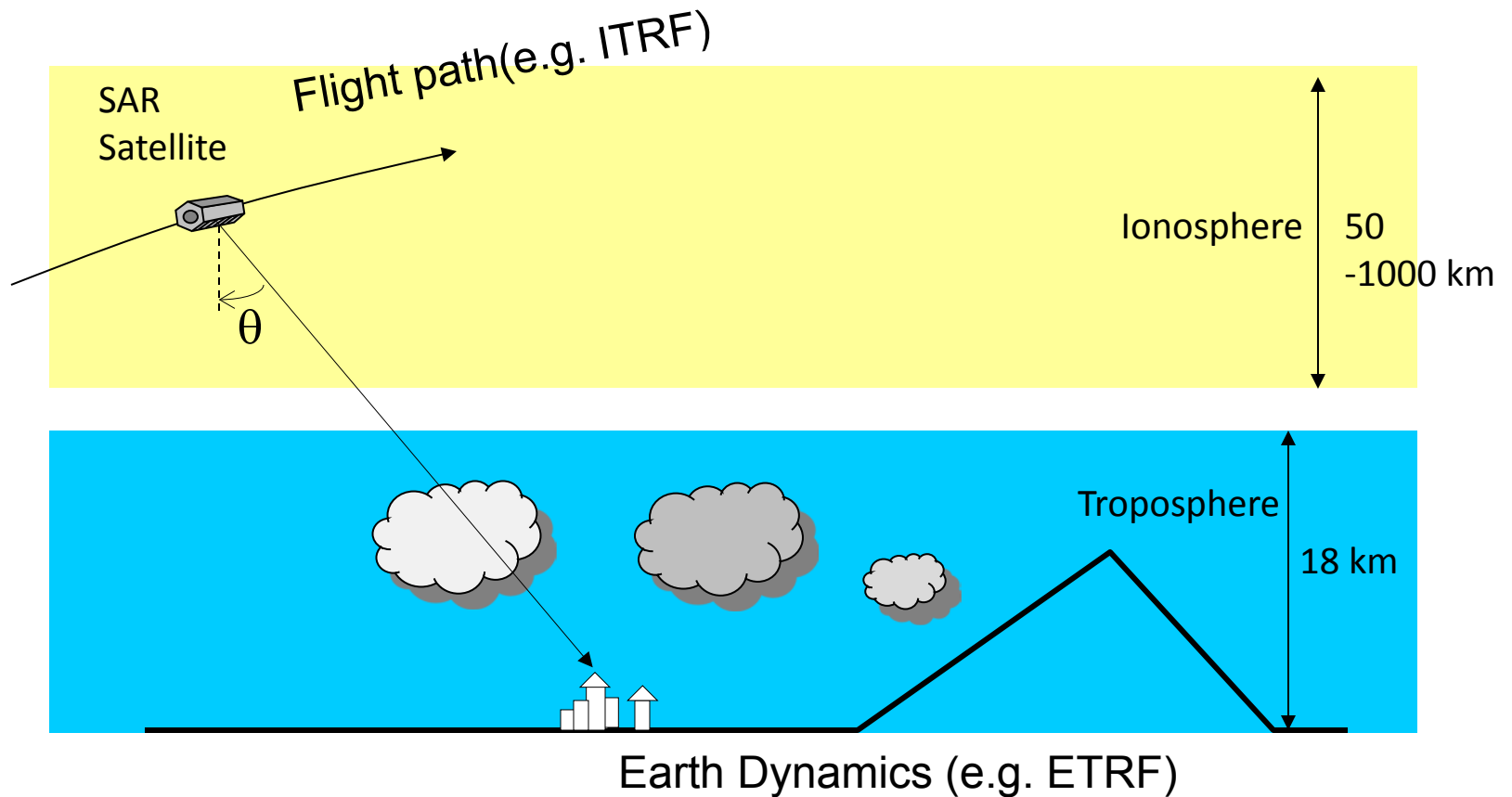
$$\varphi = 2\pi f \tau \approx 4\pi \frac{R}{\lambda}$$



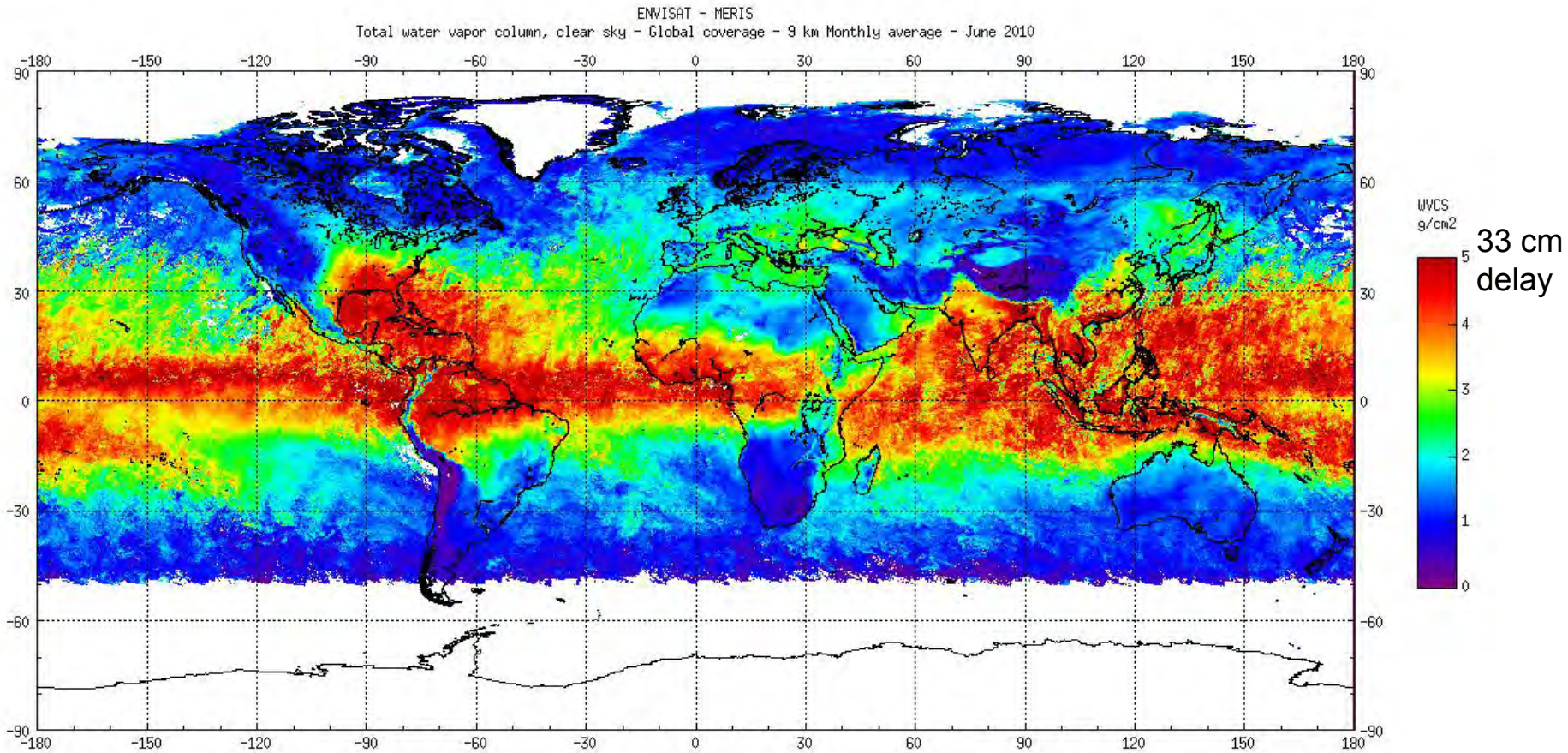
R?
c'?



SAR Signal Propagation and Coordinate Systems



Water Vapor: Spatio-Temporal Distribution

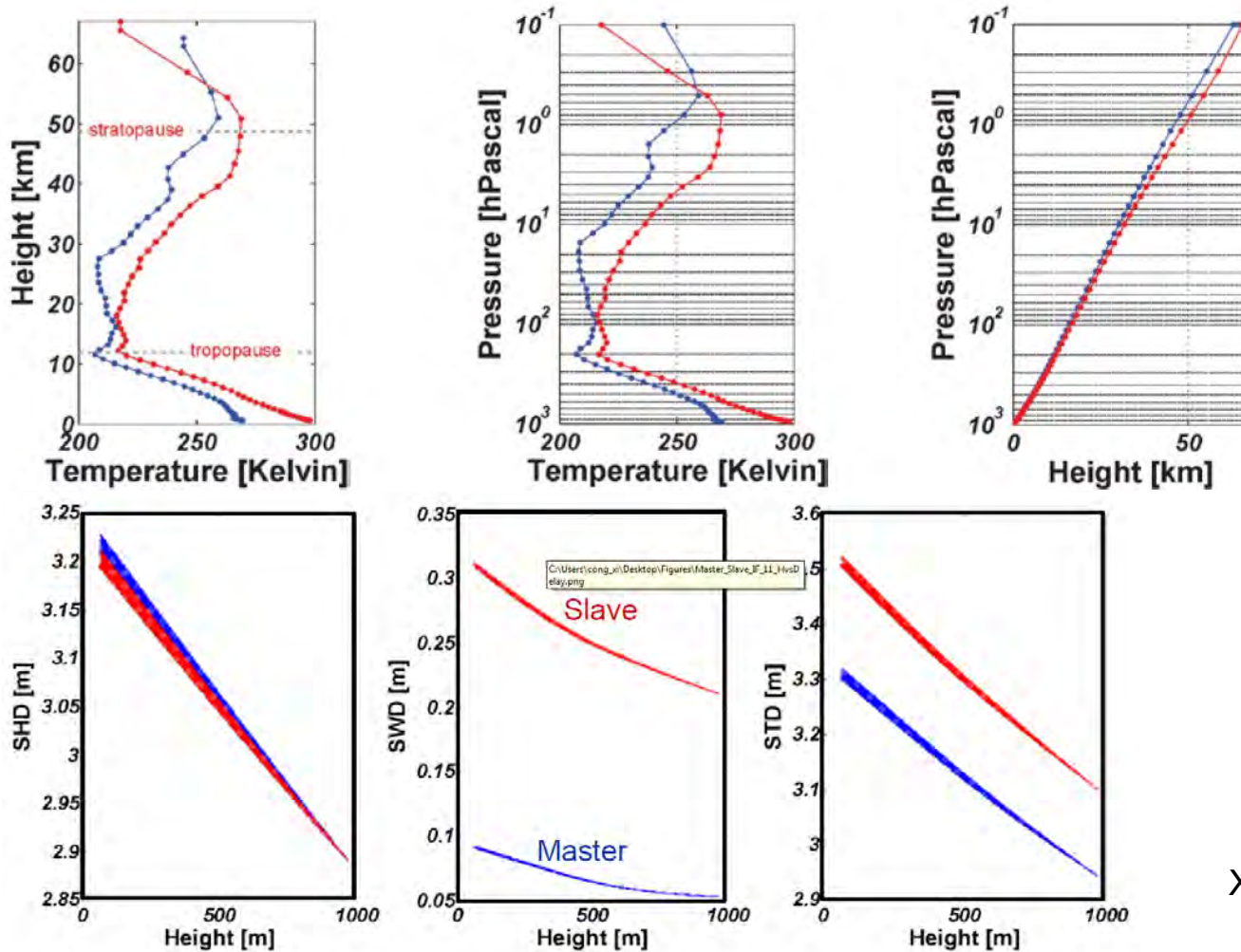


(ENVISAT Meris Clear Sky Measurements)

➔ Error of $2.5 \text{ m} \pm 20 \text{ cm}$; seasons, stratification



MultiTemporal Tropospheric Stratification from ECMWF

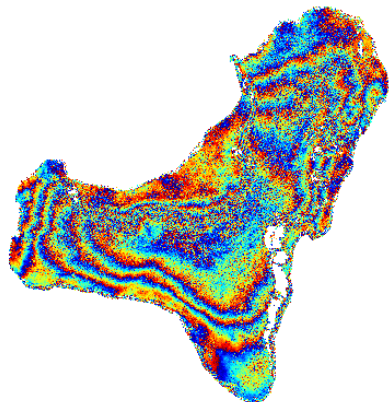


X. Cong, TUM/IMF

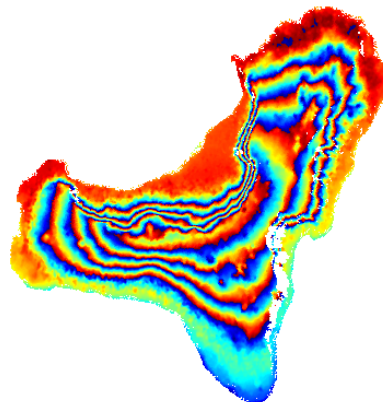


Mitigation of Atmospheric Delay Using ERA-Interim Data

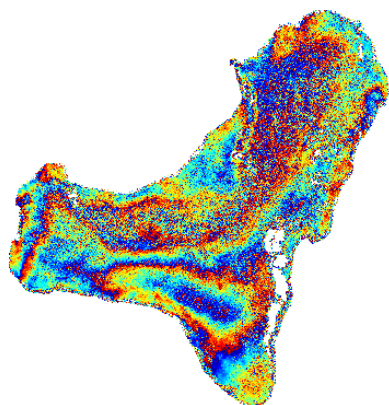
Original Phase



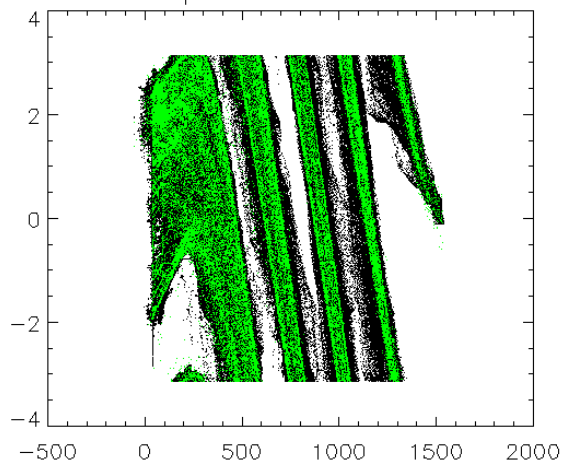
Atmospheric Phase



Corrected Phase



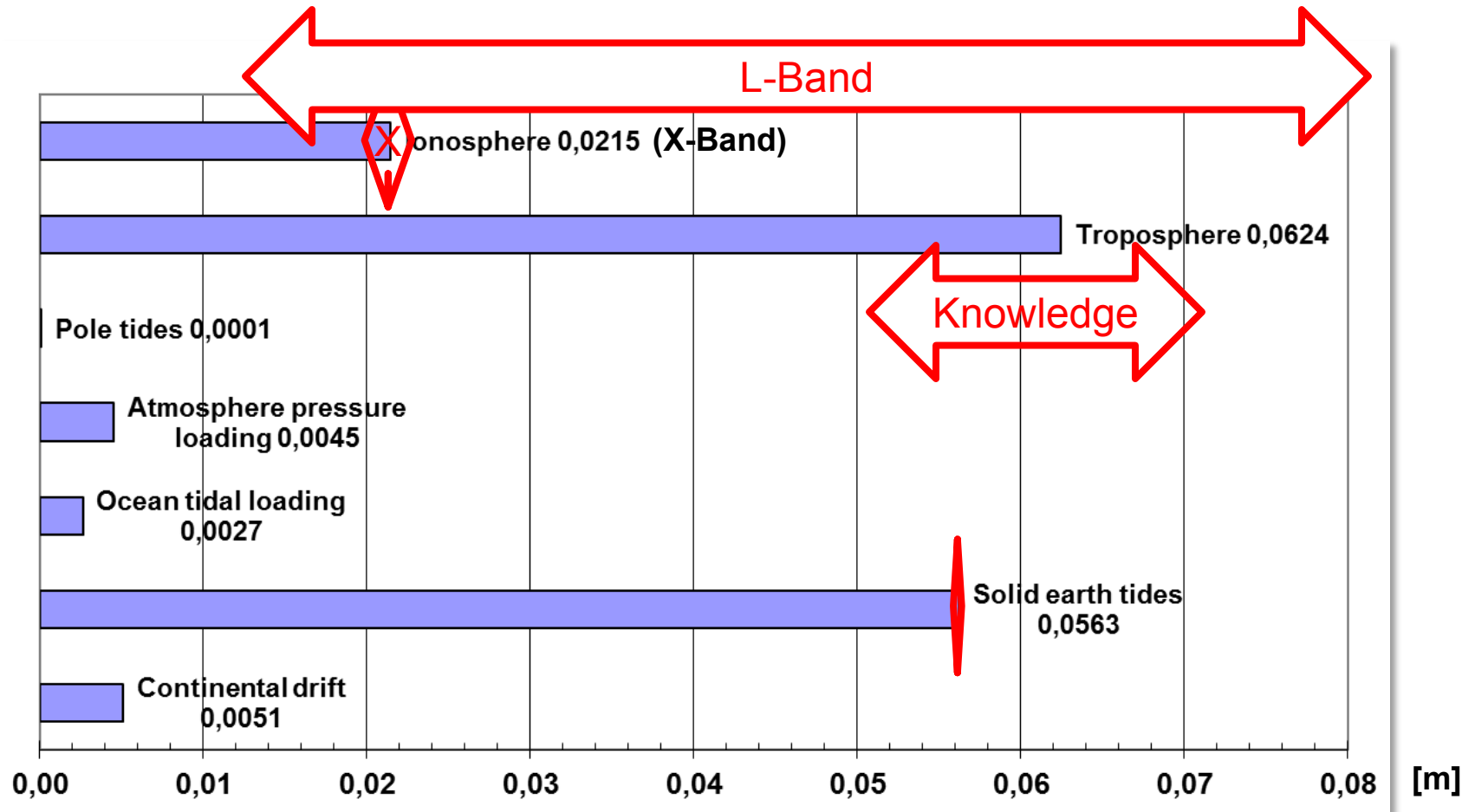
Atmospheric Phase vs. DEM



X. Cong, TUM/IMF



Summary: Geophysical Range Error Contributions



SAR Azimuth Positioning Errors

- Typical error sources
 - Not: Attitude
 - Timing synchronization between SAR and orbit metrology (GNSS)
 - SAR processor approximations (start-stop, ...)
 - ...
 - Calibration errors
 - Ionospheric gradients (C/L-Band)
 - Orbit angle error

- → 1-2 cm achievable in X-Band

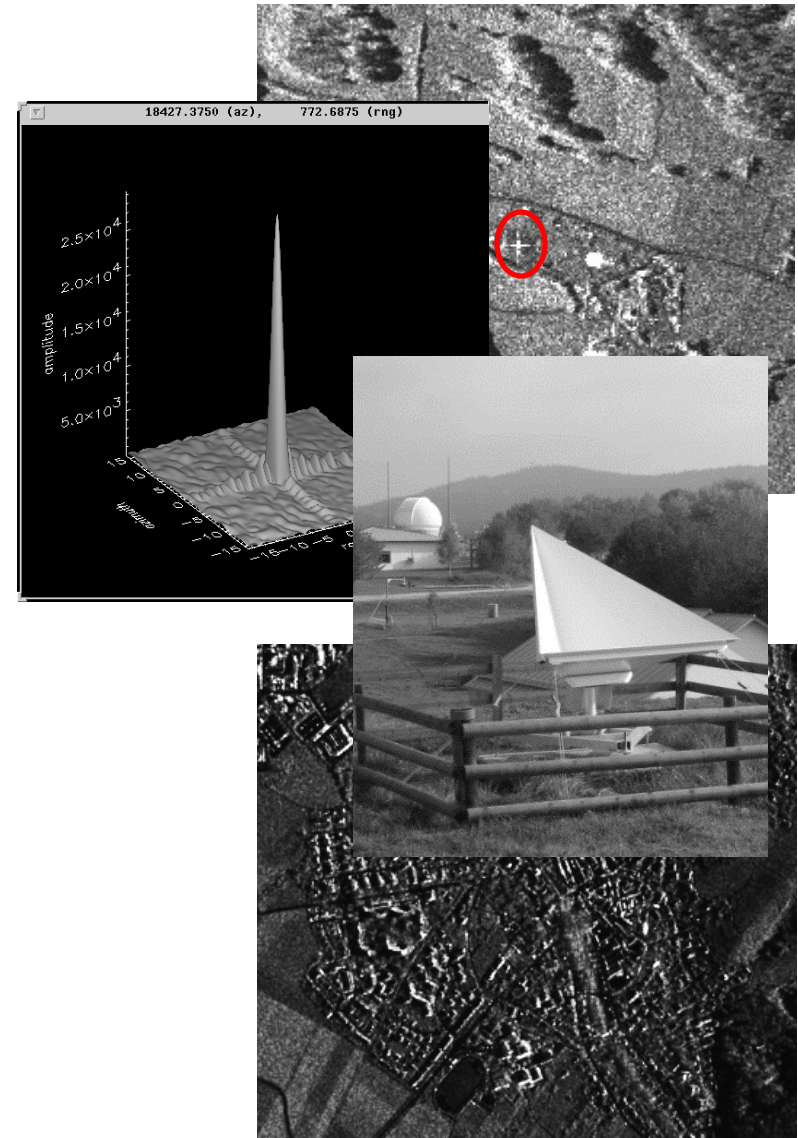


Localization of Points in Images

- Corner reflector: < 1/100 pixel accuracy achievable with point target analysis, e.g.

$$\sigma_{\text{point}} = \frac{\sqrt{3}}{\pi} \frac{1}{\sqrt{SCR}} \approx \frac{0.55}{\sqrt{SCR}} \quad [\text{res. elem.}]$$

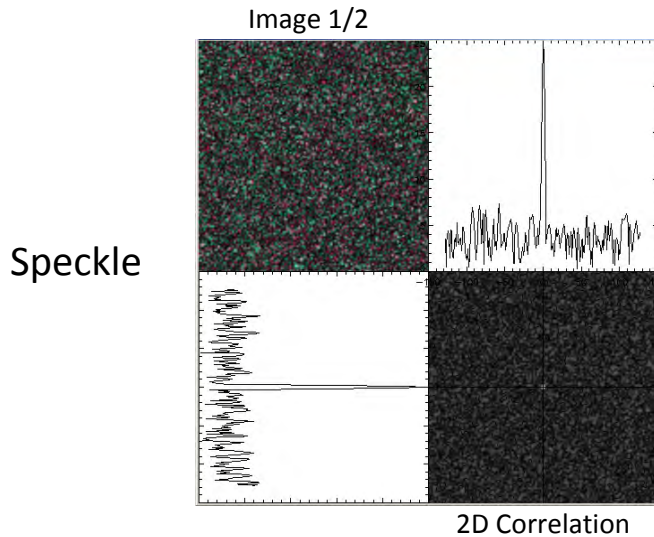
- E.g. 1.5 m CR, 1m resolution \rightarrow 2 mm error
- Persistent Scatterers: modified point target analysis
 - < 1/100 pixel accuracy (SCR)



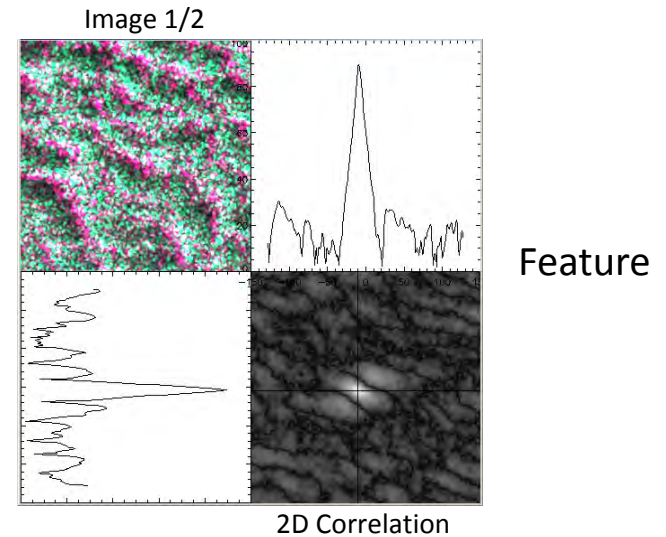
Localization of Features in Images

- Contrast / Texture: (in)coherent correlation
 - < 1/100 pixel accuracy (SNR)

$$\sigma_{area} = \sqrt{\frac{3}{2N}} \frac{\sqrt{1-\gamma^2}}{\pi\gamma}$$



E.g. coherent snow

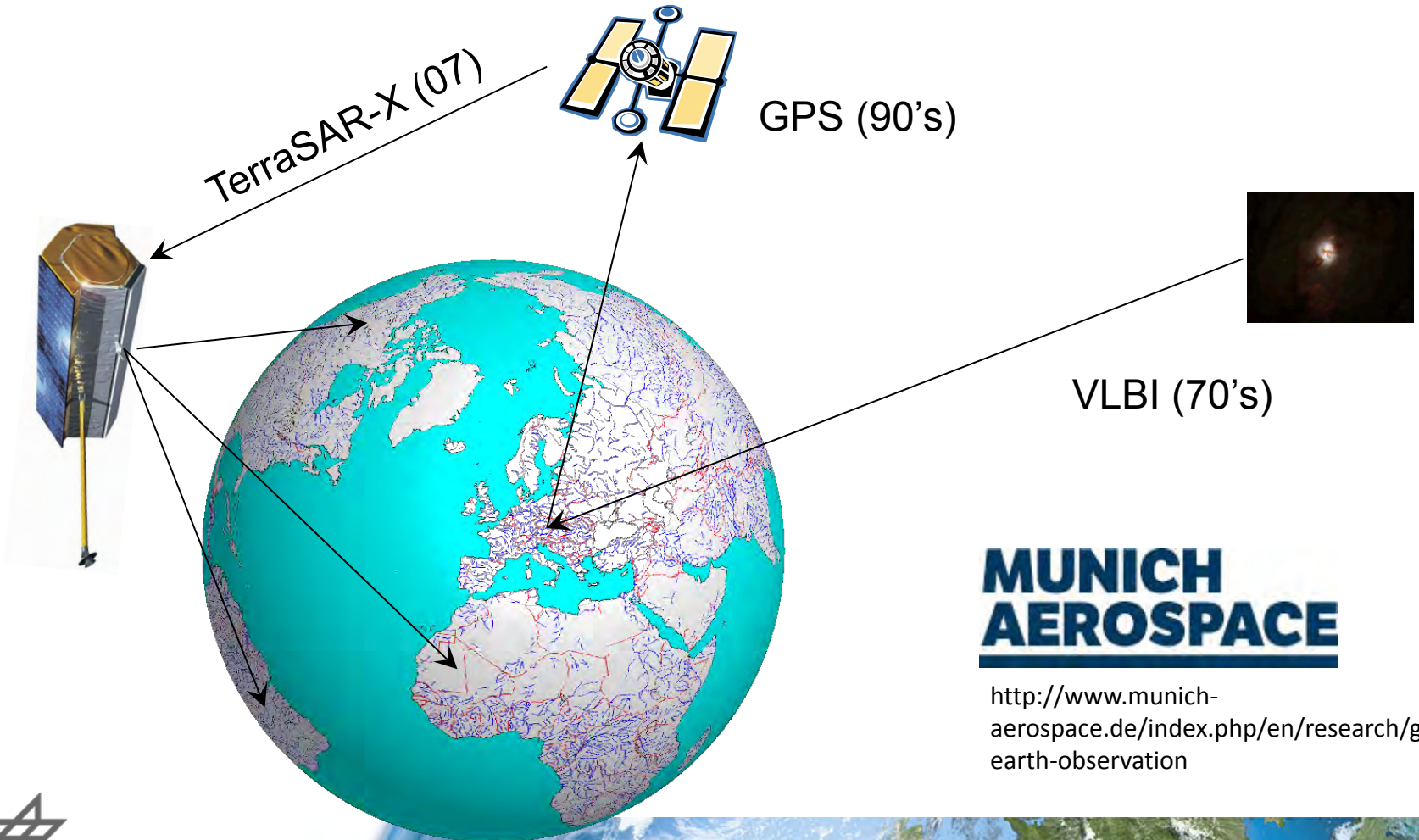


E.g. glacier crevasses



VLBI → GPS → SAR Imaging Geodesy

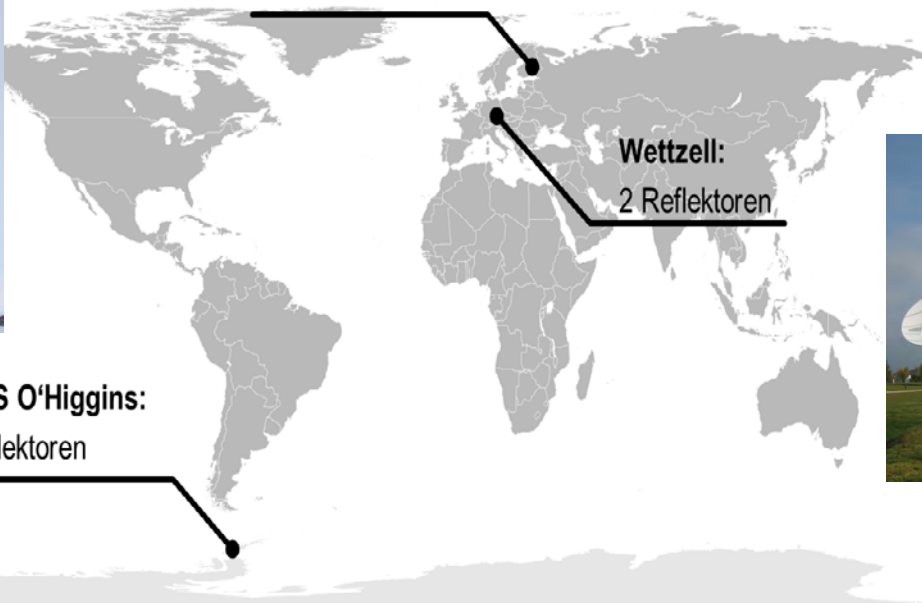
“SAR as a next generation positioning method?”



**MUNICH
AEROSPACE**

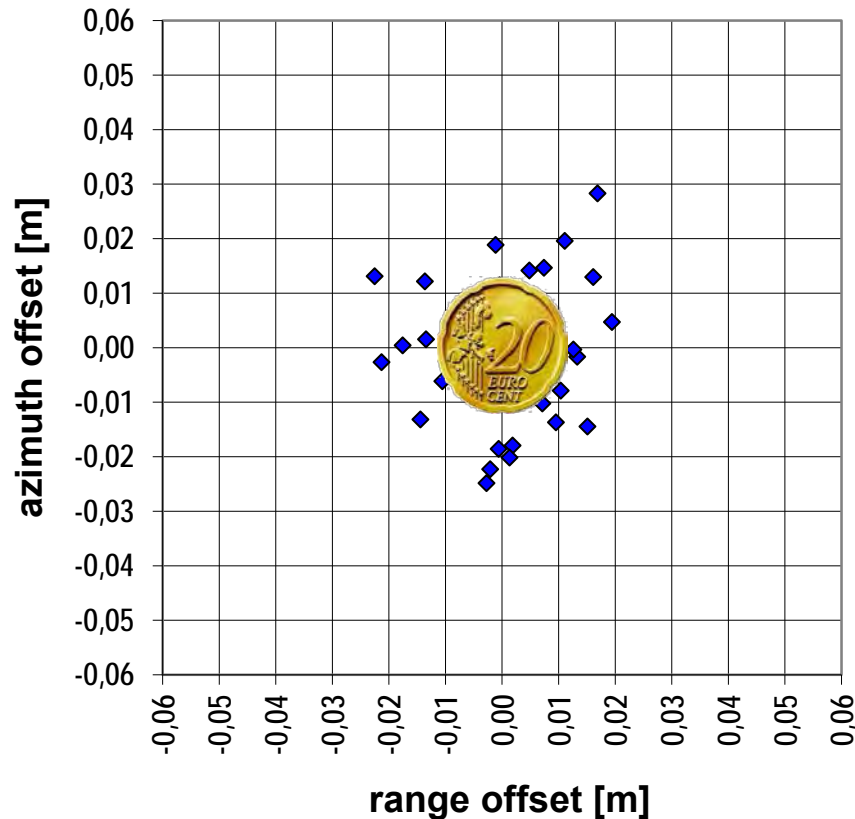
<http://www.munich-aerospace.de/index.php/en/research/geodetic-earth-observation>

DLR's Geodetic SAR-Calibration Network



TerraSAR-X Slant Range Localization Accuracy

Reflector Wetzell



After corrections of solid earth tides, atmospheric refraction (H₂O, TEC), pole tides etc.

◆ TSX (34° asc)

- ◆ Range error: $\sigma=10.8$ mm
- ◆ Az. error: $\sigma=13.0$ mm



Imaging Geodesy Application Examples

Knowledge for Tomorrow

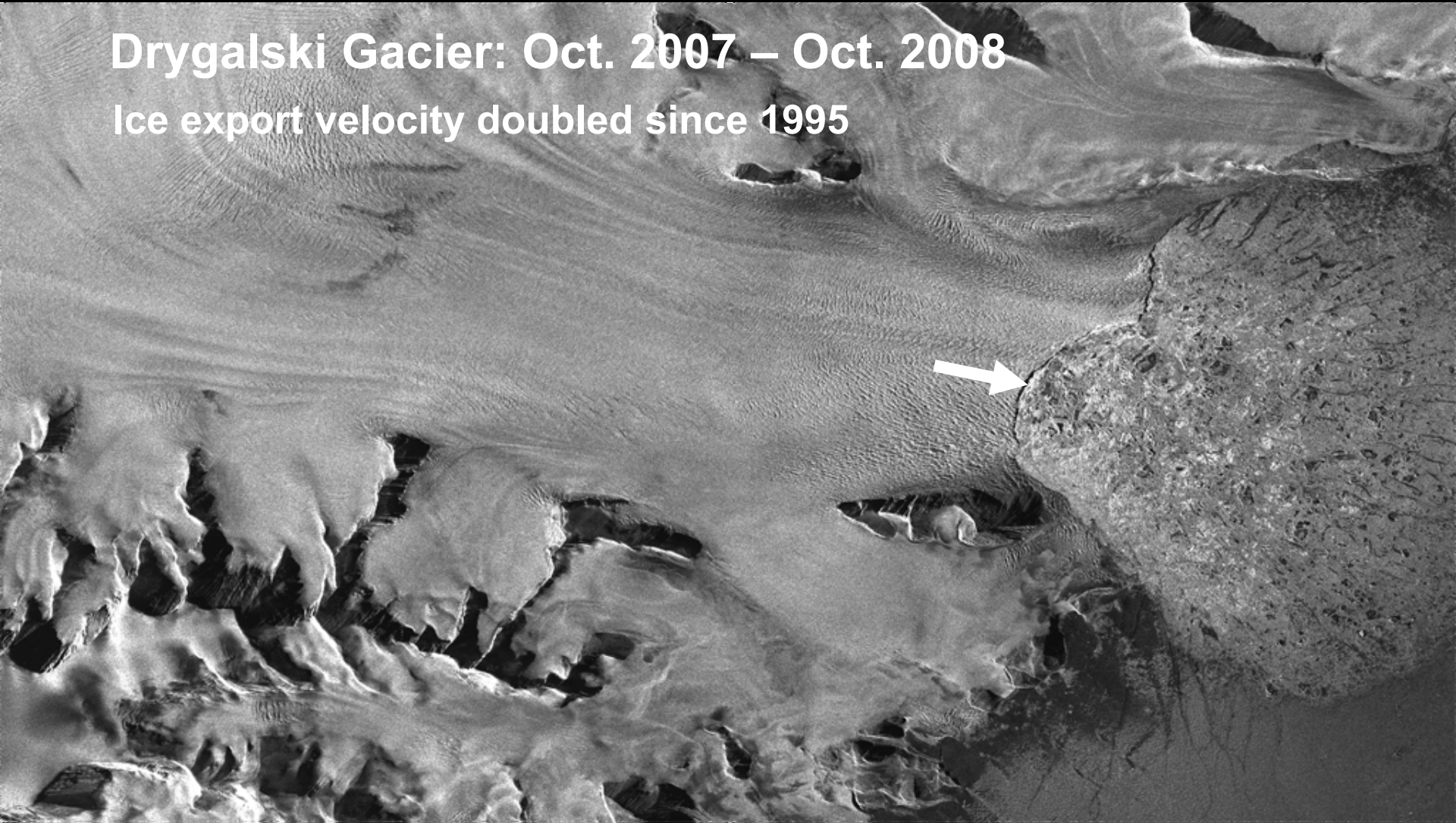


Velocity Measurements without GCPs



Drygalski Gacier: Oct. 2007 – Oct. 2008

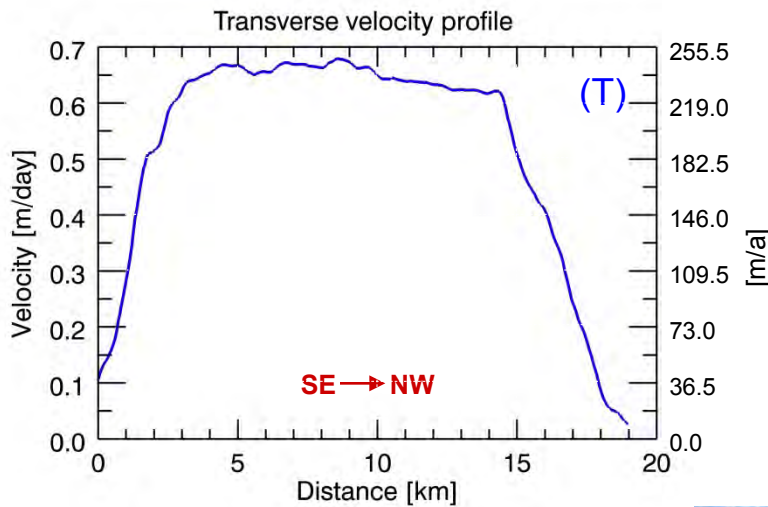
Ice export velocity doubled since 1995



Mass changes of outlet glaciers along the Nordensjököld Coast, northern Antarctic Peninsula, based on TanDEM-X satellite measurements, H. Rott et al, Geophysical Research Letters, 2014.

Video: M. Eineder

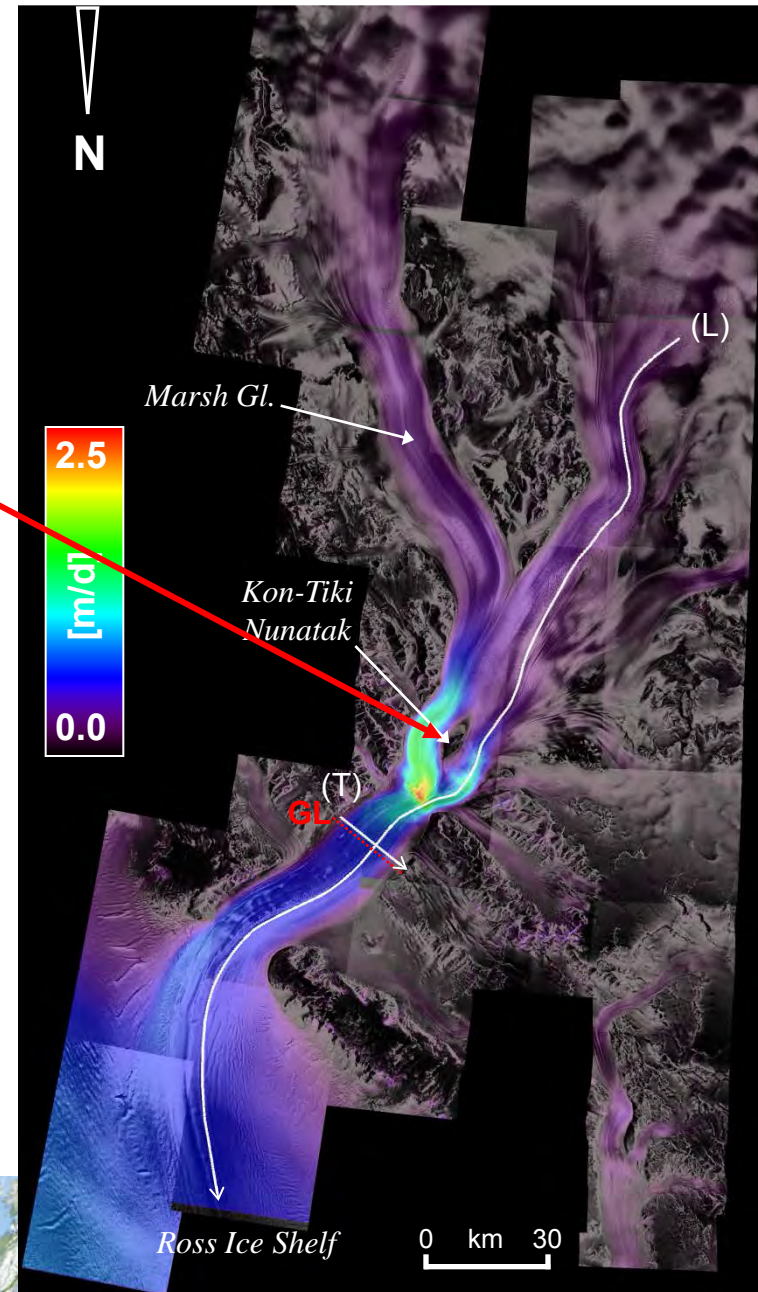
Ice Surface Velocity from TerraSAR-X Nimrod Glacier



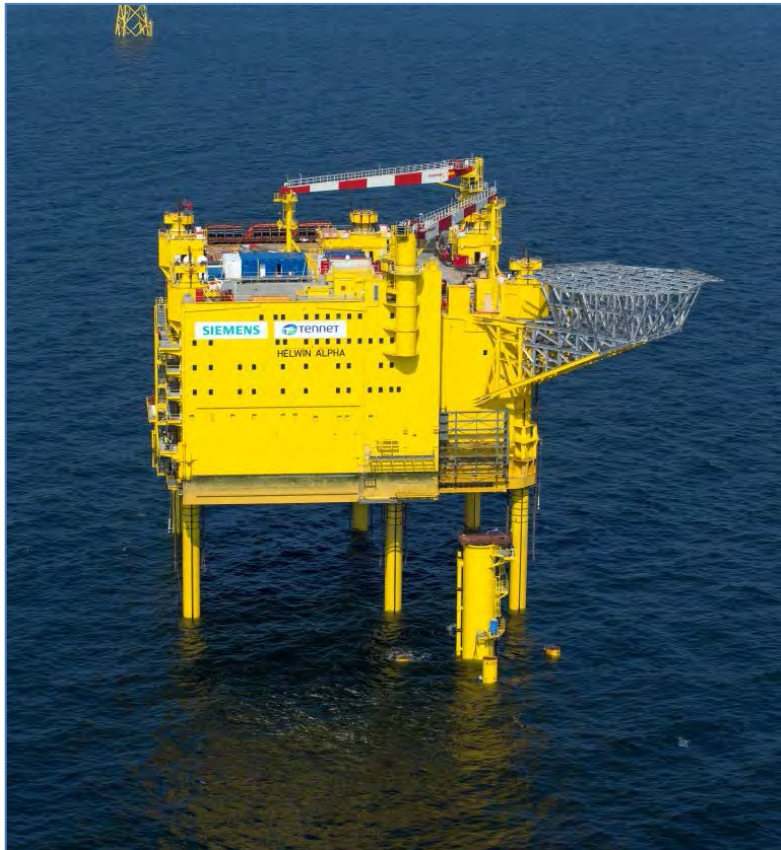
→
Plug-like
shape:
strong side
drag



W. Abdel Jaber,
D. Floricioiu, DLR-IMF



Applications: Offshore Platform Monitoring. Test site

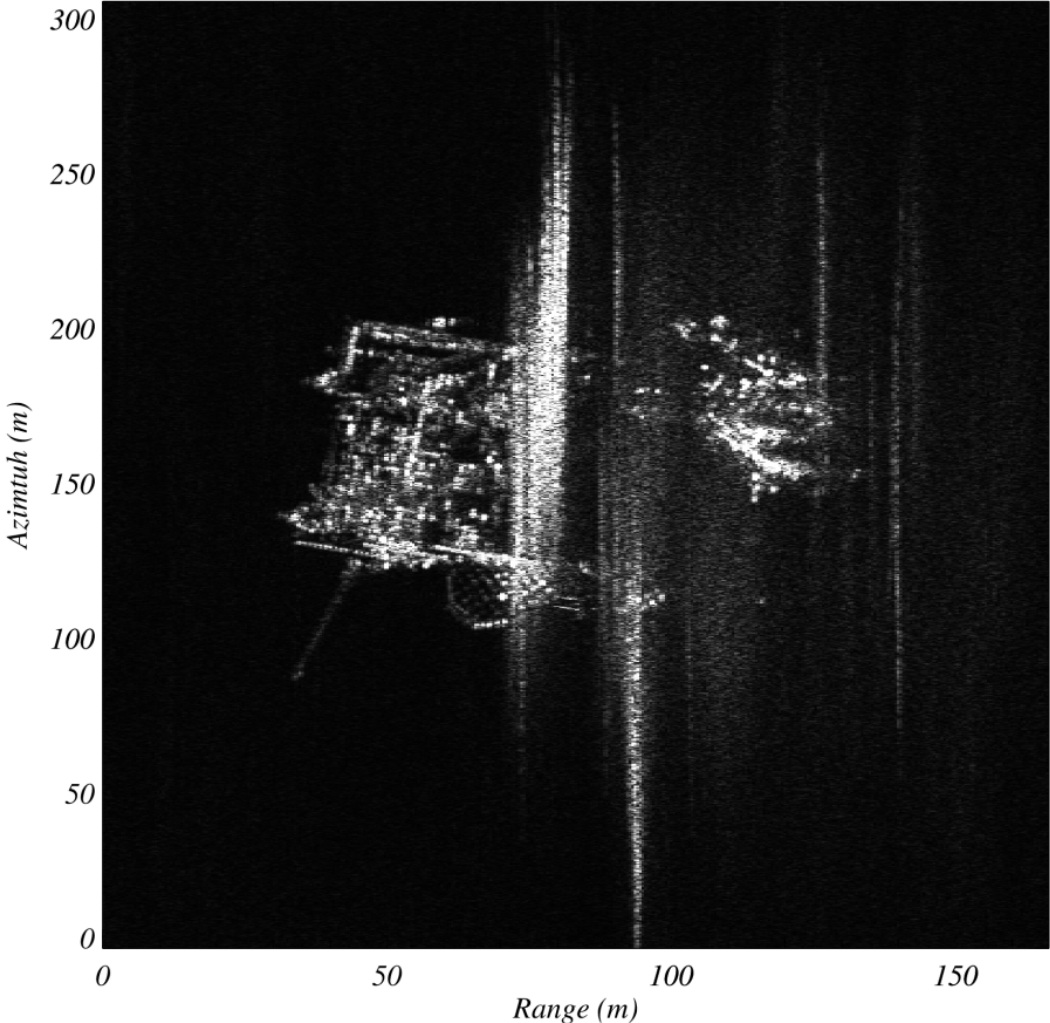


- Helwin1: seabed attached platform installed by Siemens in the North Sea in 2013
- Converts AC power generated by wind farms into low-loss DC for transmission to land
- Closest land more than 40 km away

Duque S. et al., Accurate Measurements Using TerraSAR-X And TanDEM-X Data Without Any Reference, IGARSS 2014, DLR-IMF



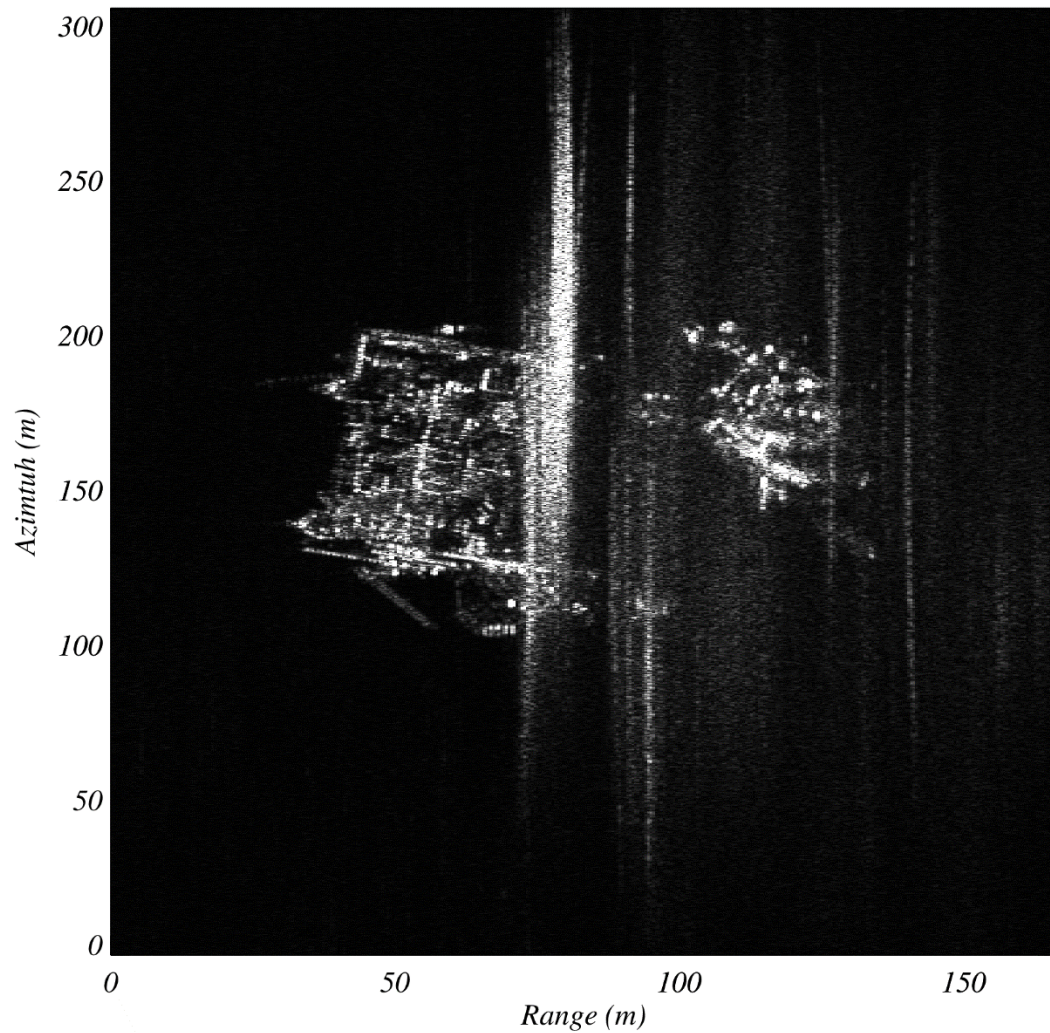
Master Image



TerraSAR-X
Staring
Spotlight
4.11.2013



Slave Image

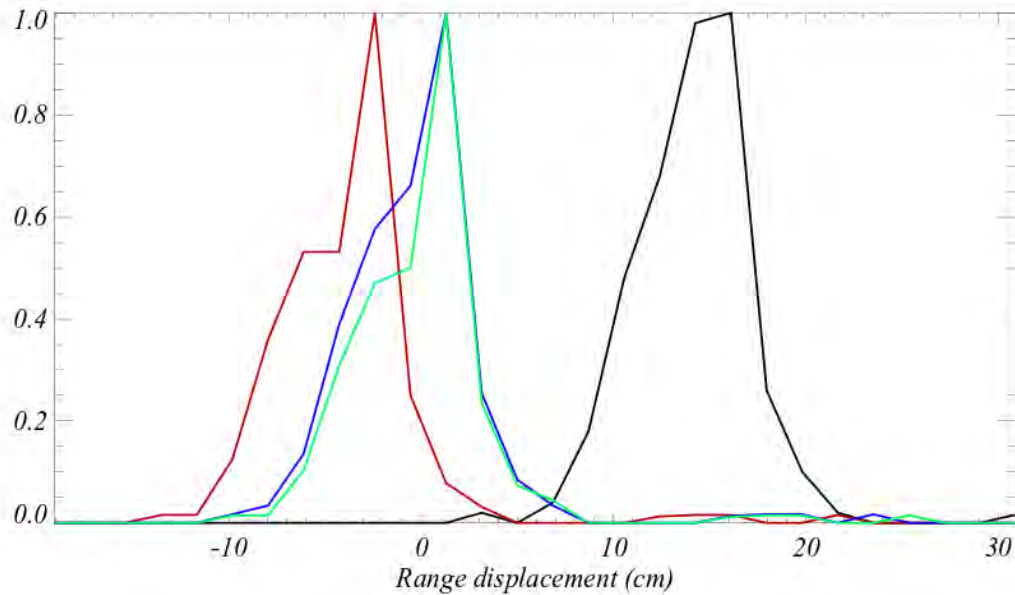


TerraSAR-X
Staring
Spotlight
15.11.2013



Applications: Offshore Platform Monitoring

Range Histogram



- Incoherent Cross Correlation (ICC)
- ICC + tropo
- ICC + tropo + SET
- ICC + tropo + SET + TOL

$\mu_{rg} = 0.7 \text{ cm}$
 $\sigma_{rg} = 1.1 \text{ cm}$

Duque S. et al., Accurate Measurements Using TerraSAR-X And TanDEM-X Data Without Any Reference, IGARSS 2014, DLR-IMF



3D Localization of Reflectors using Stereo-SAR

A lamp pole near the central railway station

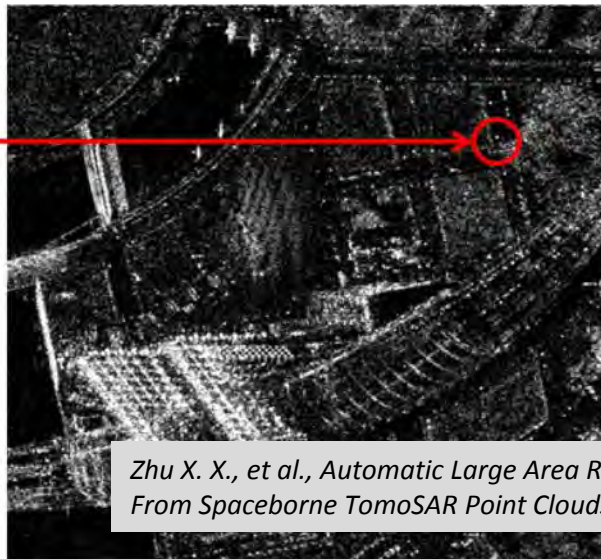
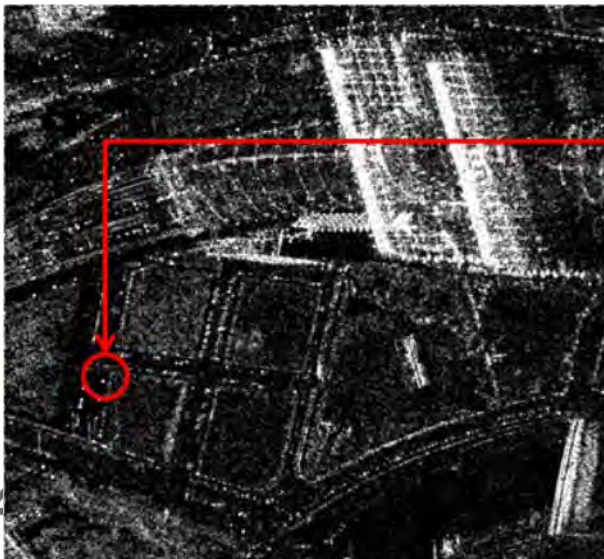
Coordinates in the ITRF 2008 reference frame:

$$x = 3783630.014 \pm 0.010\text{m};$$

$$y = 899035.0040 \pm 0.010\text{m};$$

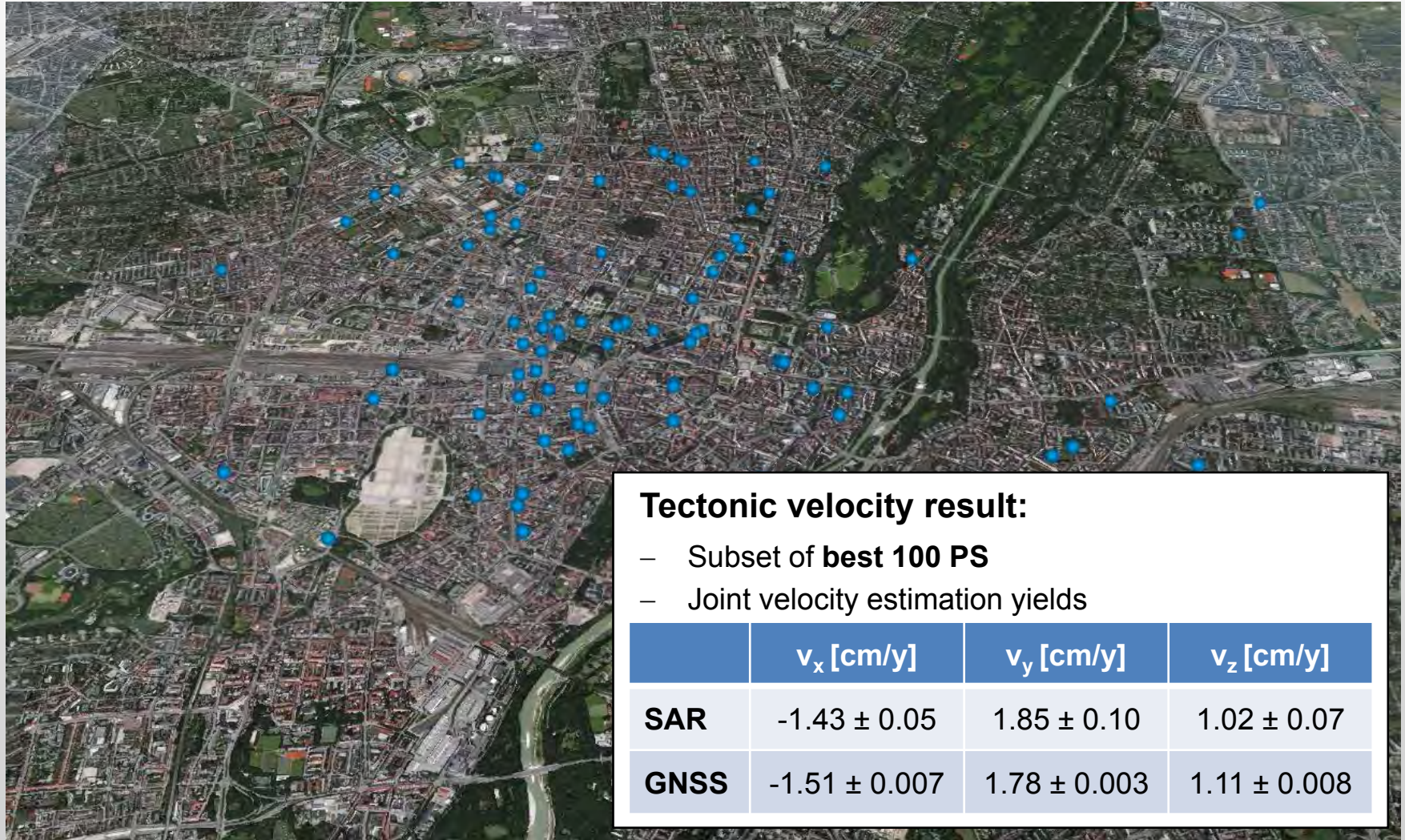
$$z = 5038487.589 \pm 0.011\text{m}.$$

Diameter of ca. 20cm \rightarrow systematic bias, still to be considered!



Zhu X. X., et al., Automatic Large Area Reconstruction Of Building Façades From Spaceborne TomoSAR Point Clouds, IGARSS 2014, DLR-IMF

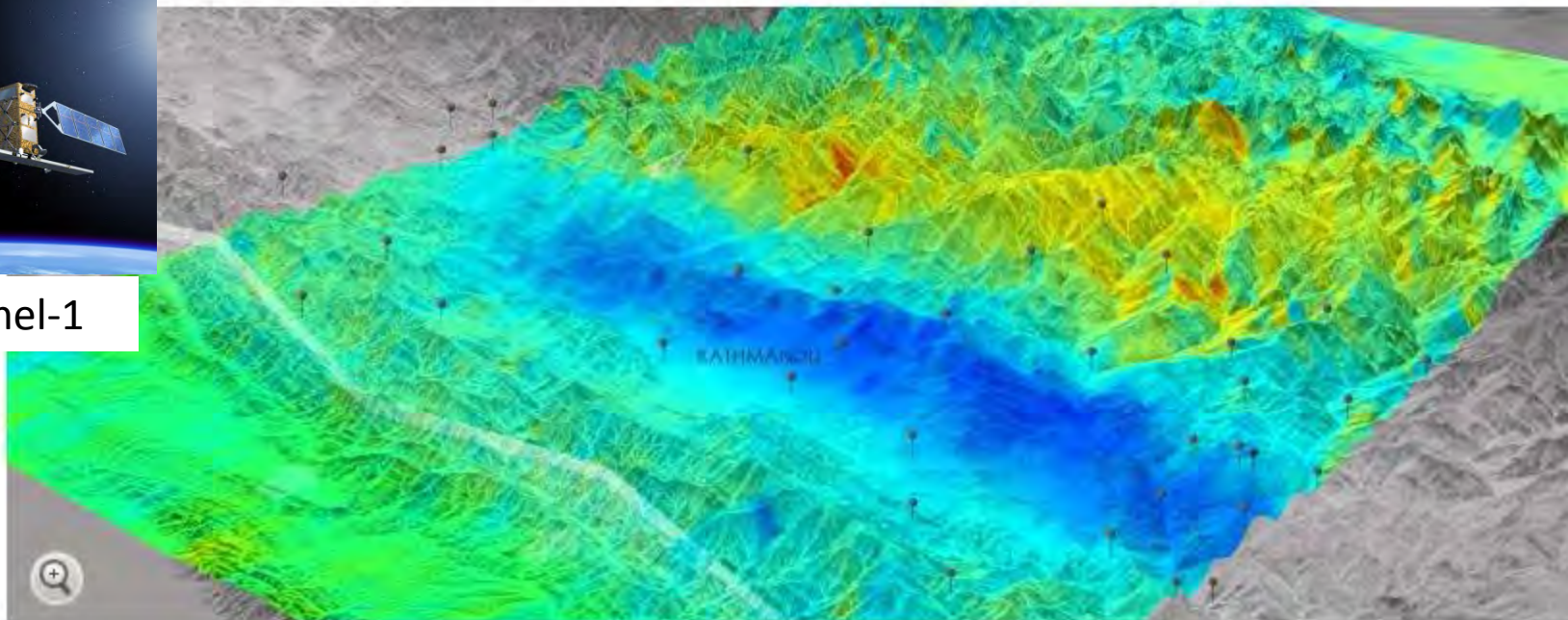
- Geodetic Stereo SAR for about **1200 PS** in the city of Munich (0.2 m)



Satellitenbild der Woche: Wie das Erdbeben Nepal verändert



Data: Sentinel-1



Bodenveränderung nach Erdbeben: Blau zeigt Hebung, Gelb und Rot Senkung

Rodriguez

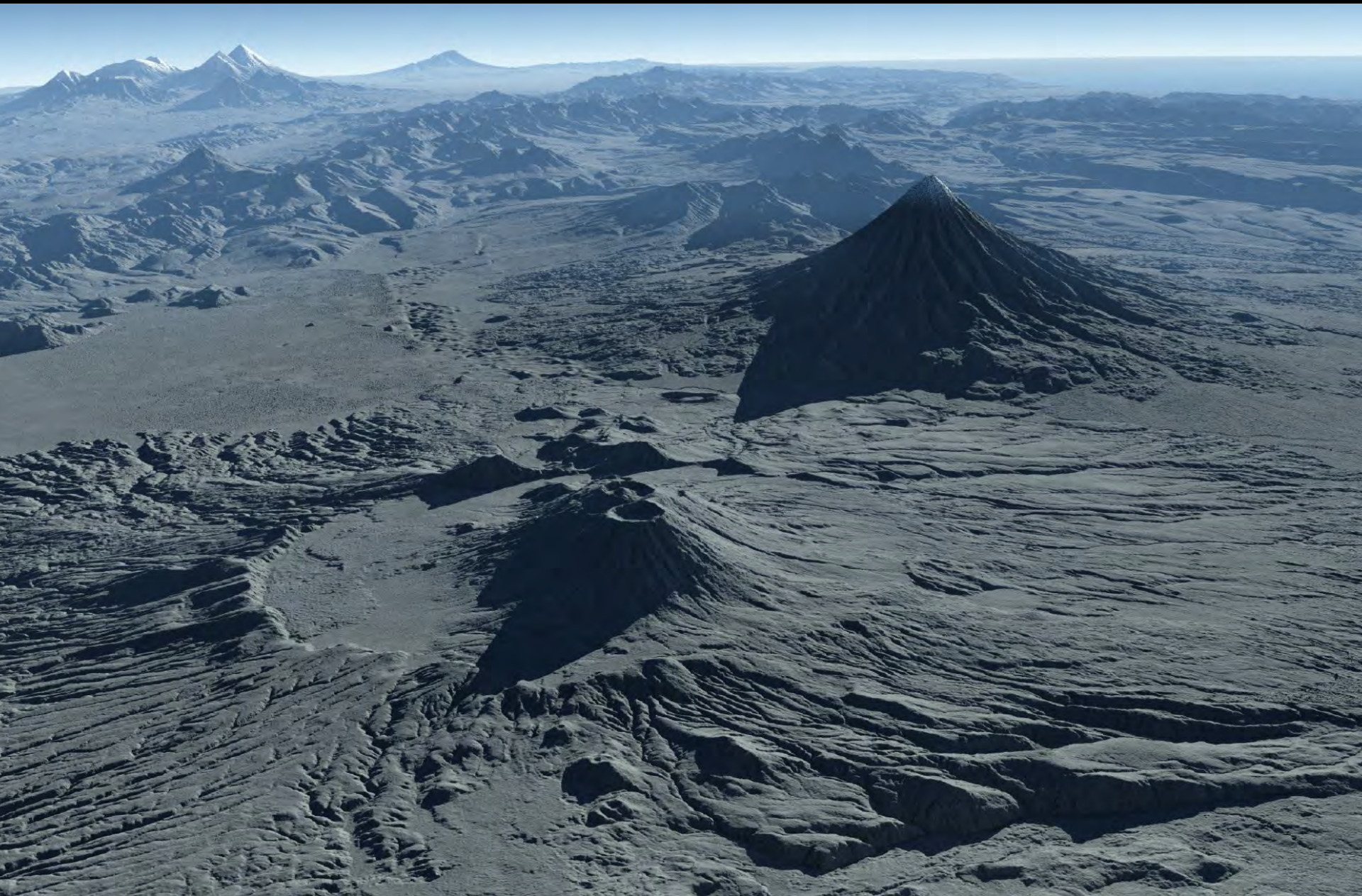
Das schwere Erdbeben hat katastrophale Folgen für Nepal - und das Land gravierend verändert. Ganze Landstriche wurden höher und tiefer gelegt.

TanDEM-X DEMs

Knowledge for Tomorrow





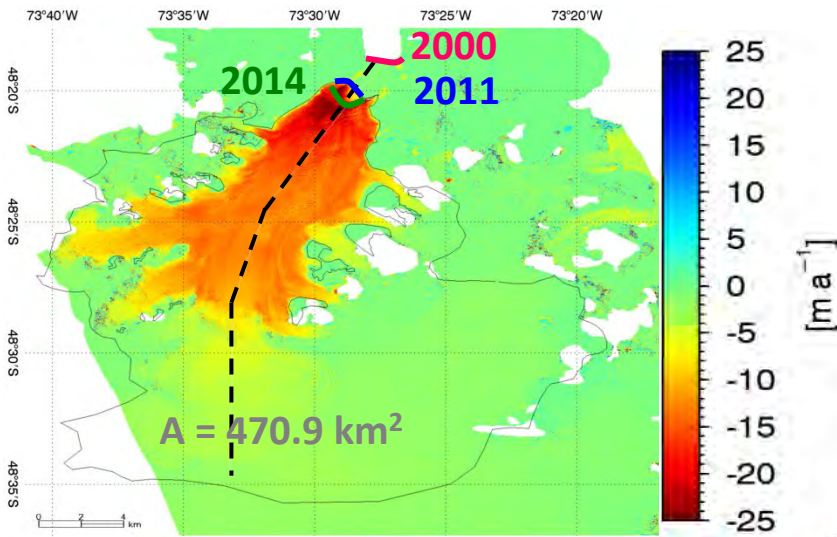


Mass balance of glaciers from DEM differencing

$$\frac{dM}{dt} = \int_A \rho \frac{\Delta h}{\Delta t} dA$$

Surface elevation change rate

TanDEM-X 21.04.2014 - 9.05.2011



J. Montt, South Patagonia Icefield



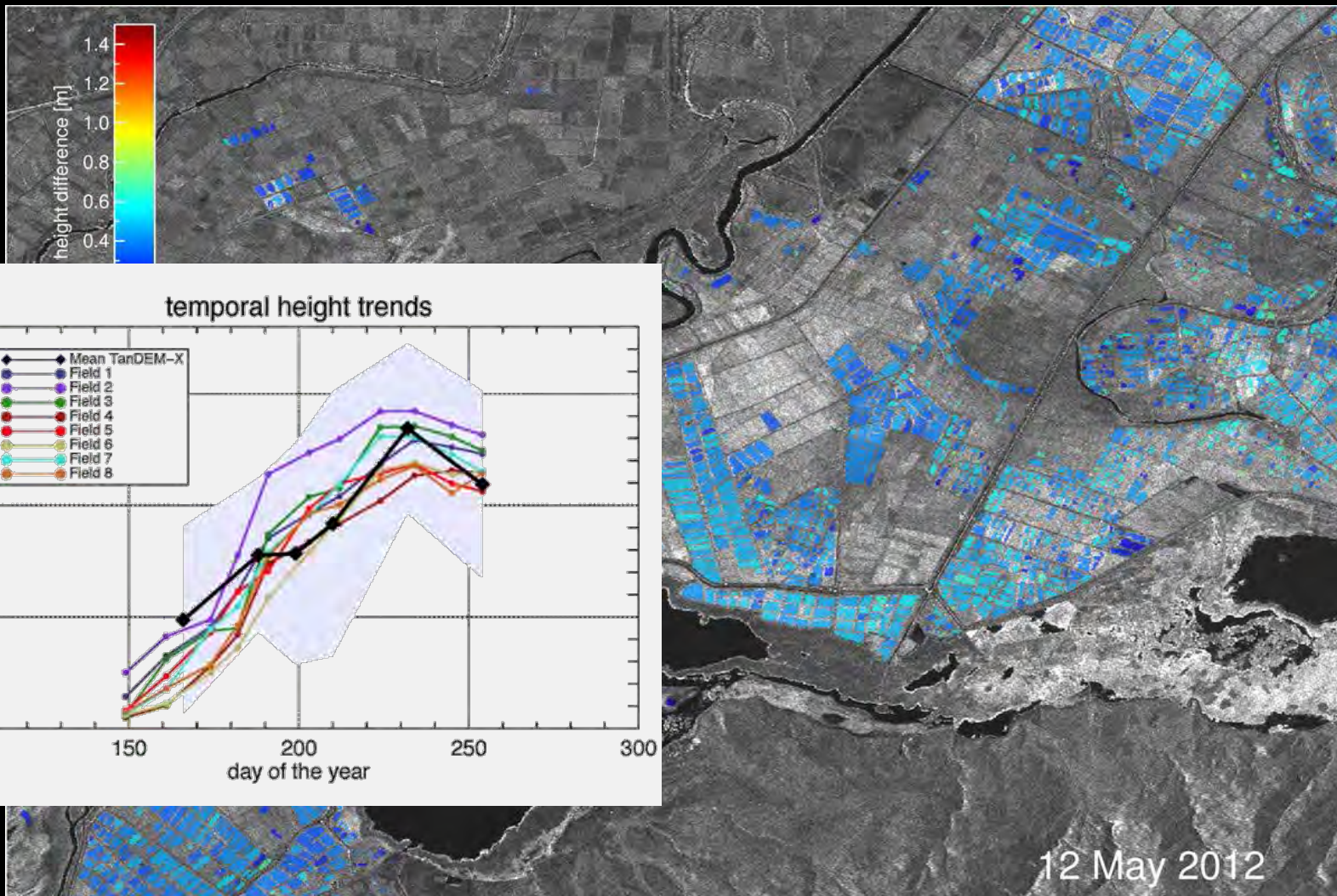
Acceleration of surface lowering



D. Floricioiu, W. Abdel Jaber, DLR-IMF



Rice Growth Monitoring using MultiTemporal DEMs



High Resolution SAR Interferometry

Knowledge for Tomorrow



Case Study: Berlin, Central Railway Station

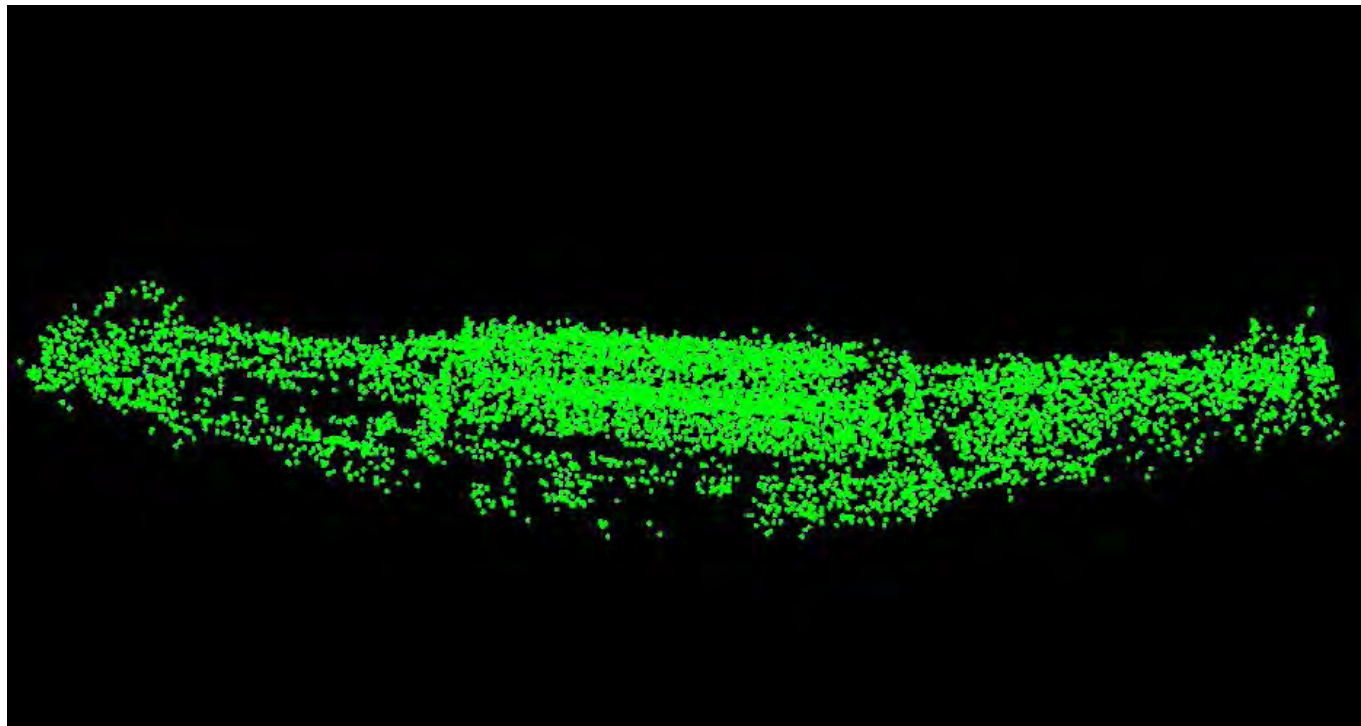
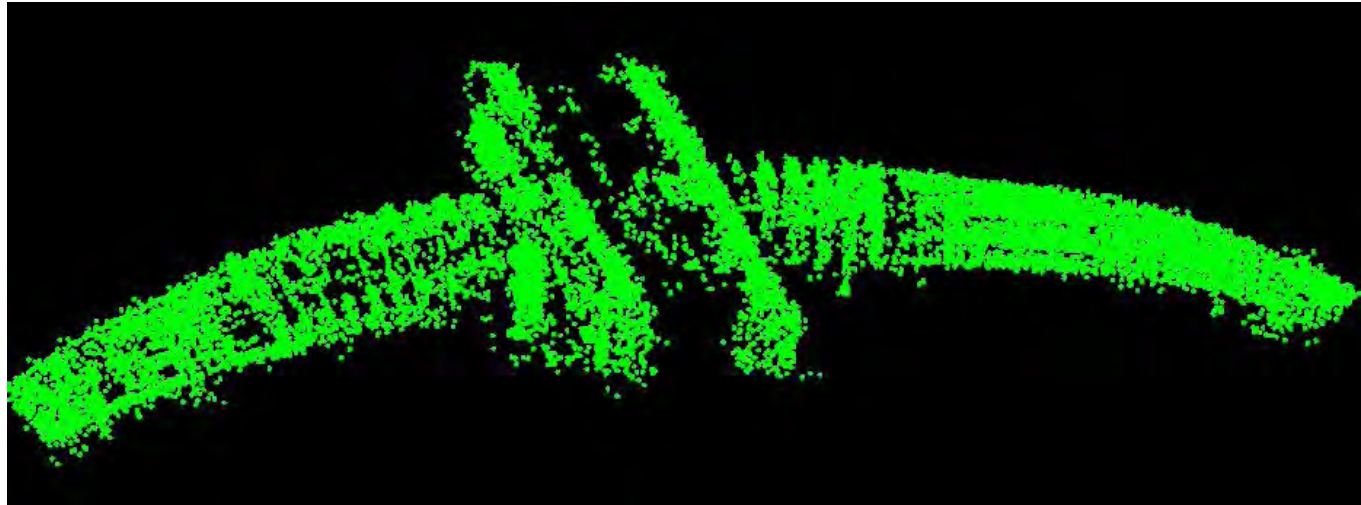


TerraSAR-X



Google Earth





S. Gernhardt TUM



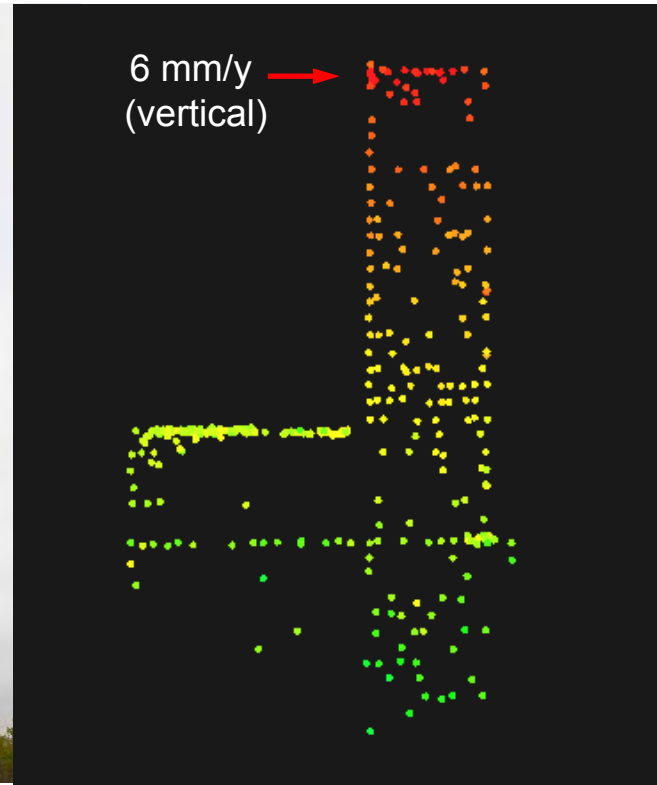
Height Dependent Motion on Buildings (I)

SV Verlagsgebäude, Munich

- Recently built steel-concrete building
- Height dependent linear motion



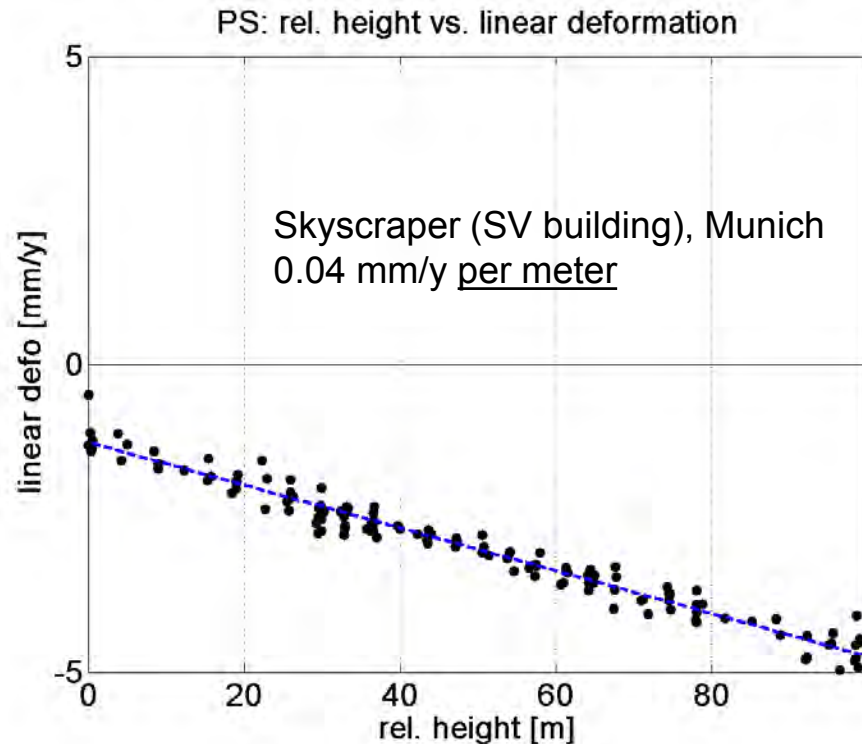
Photo: M. Eineder



Color: Linear deformation
S. Gernhardt, TUM
(2014)



Height Dependent Motion on Buildings (II)



Reason: compaction of concrete (dehydration & creeping) !

Gernhardt G, Bamler R (2015) Structural Deformation and Non-seasonal Motion of Single Buildings in Urban Areas Revealed by PSI. Proc. Joint Urban Remote Sensing Event, Lausanne, submitted.

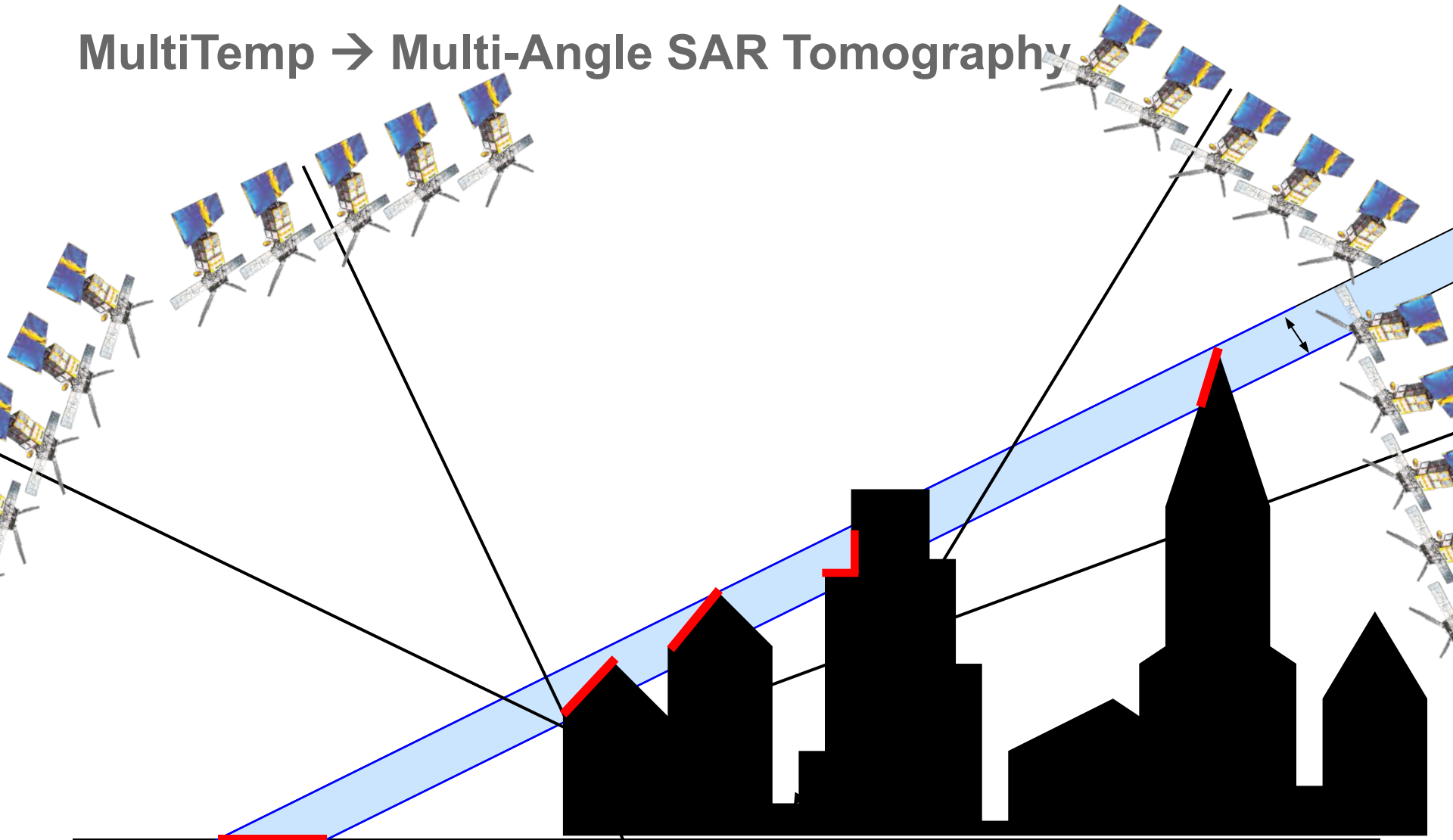


SAR Tomography

Knowledge for Tomorrow



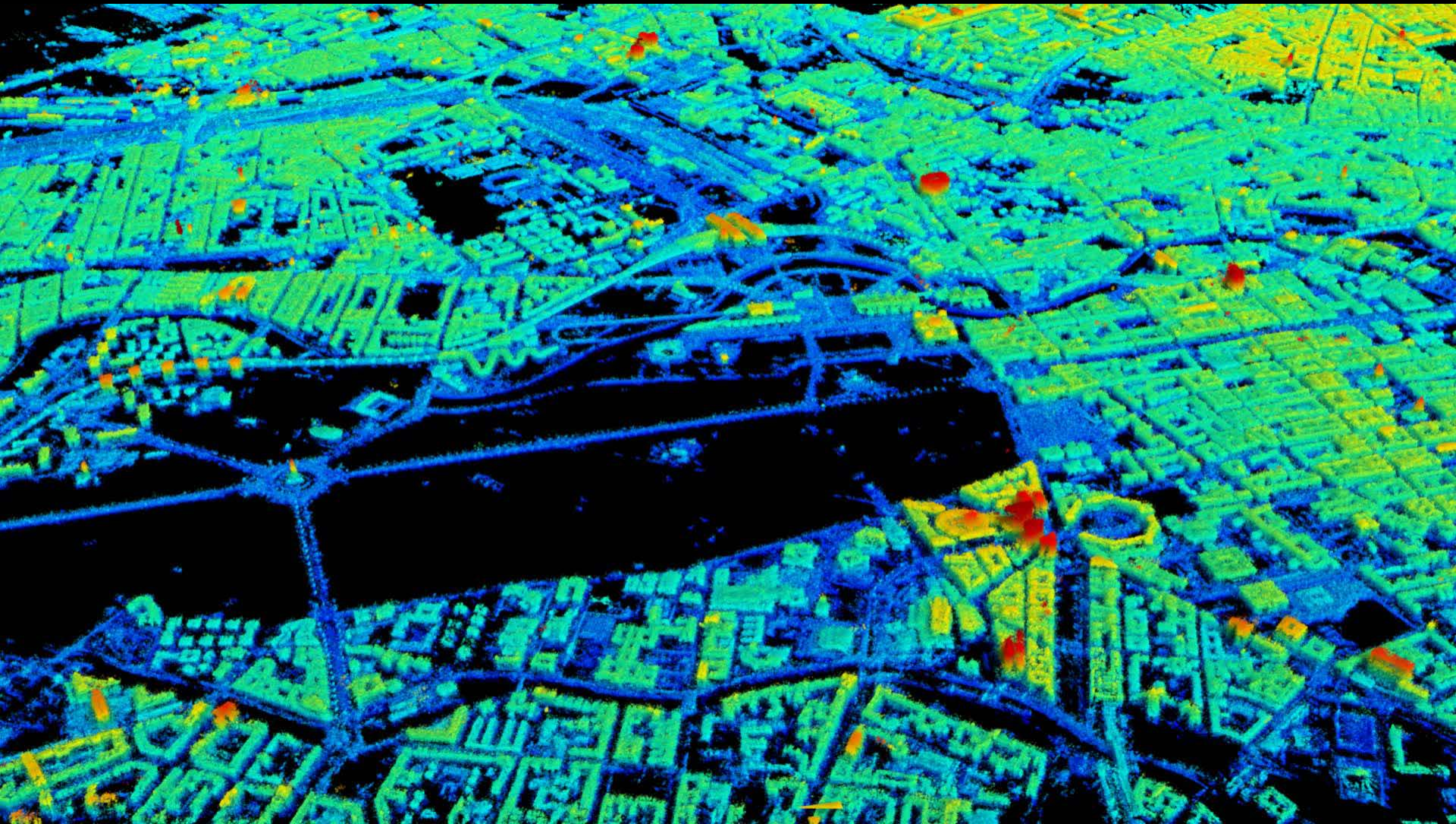
MultiTemp \rightarrow Multi-Angle SAR Tomography



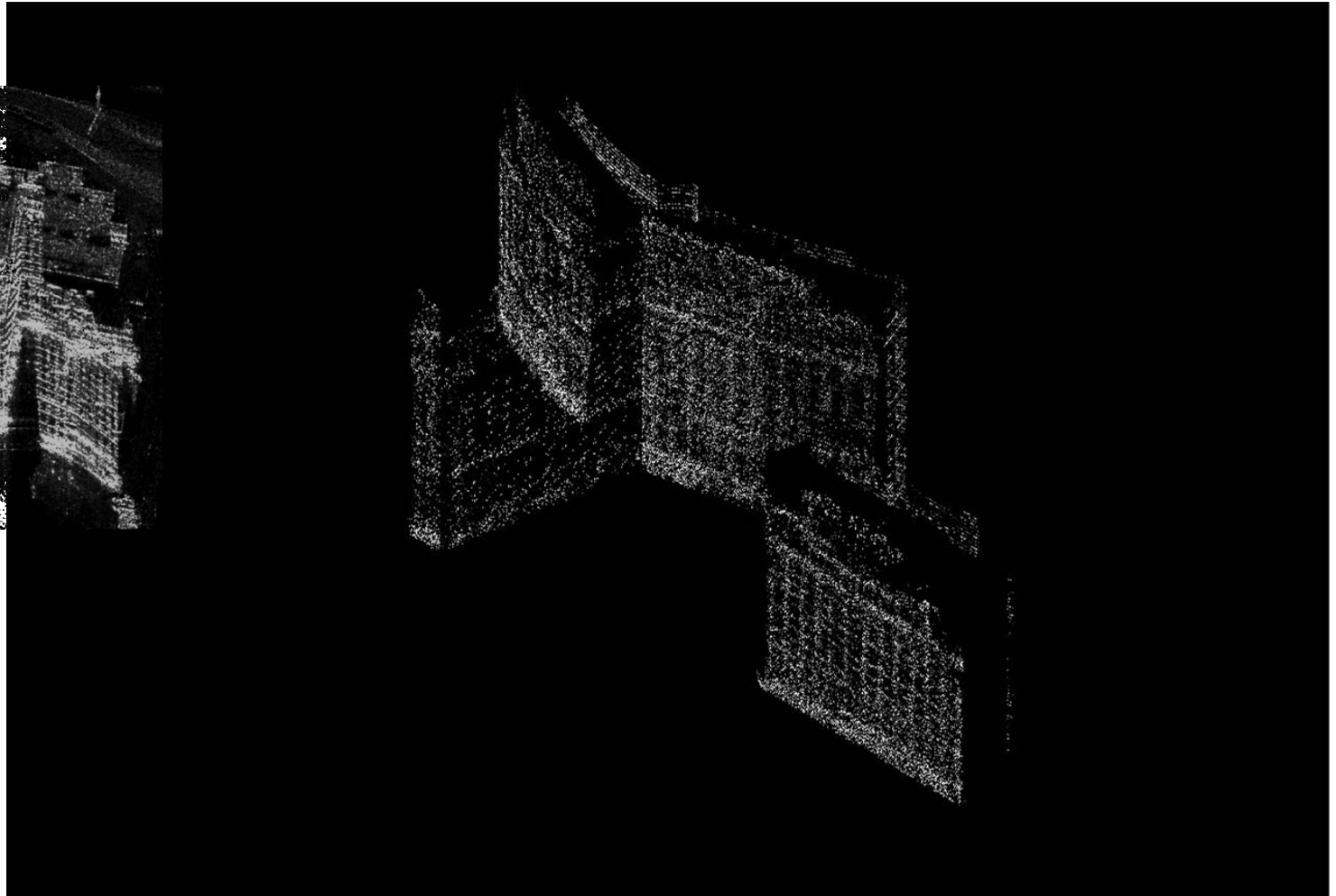
LOS



Tomographic SAR Imaging of Urban Areas (>600 img.)



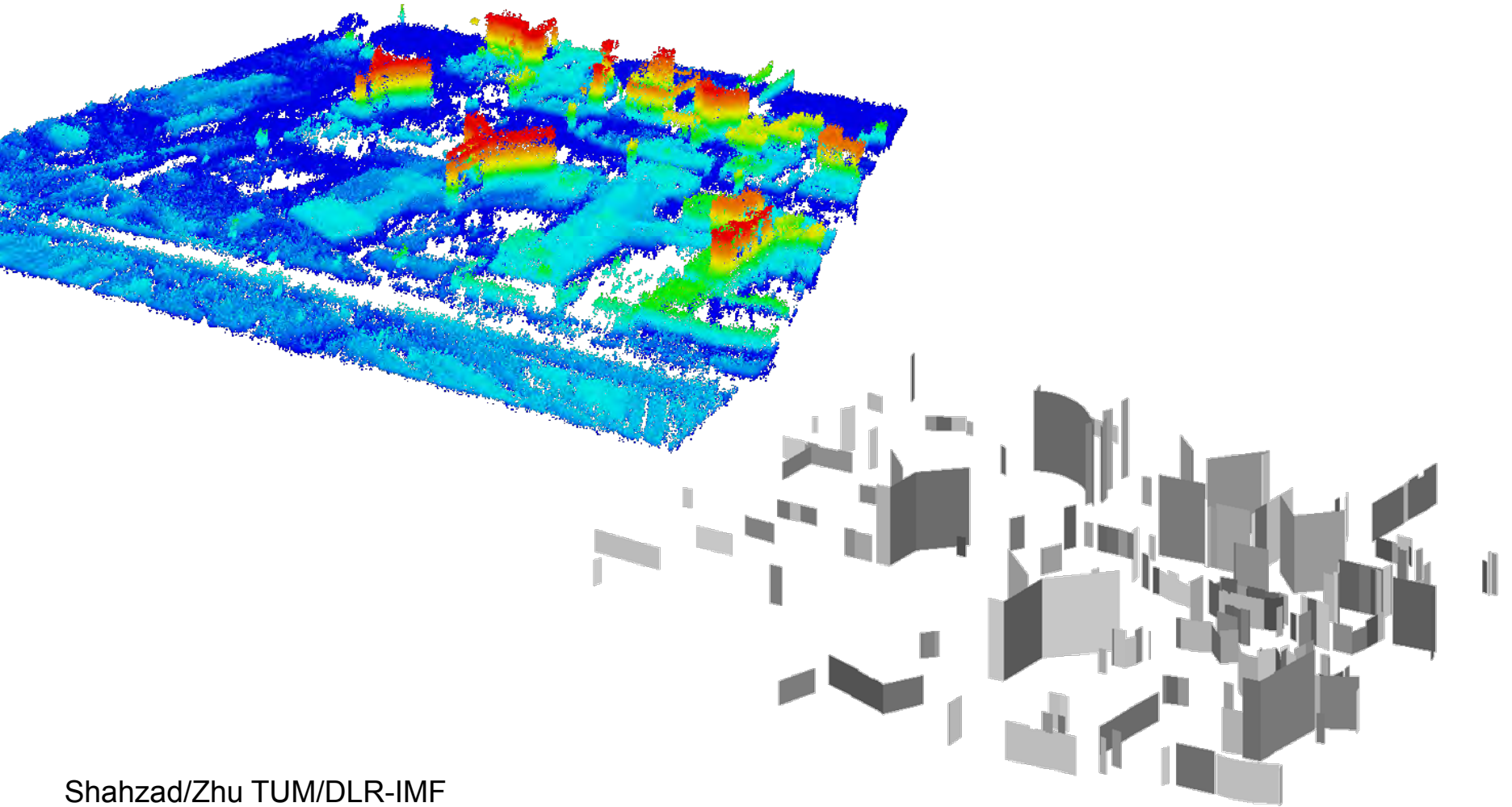
2D → 3D SAR: Separation of Wall / Ground Reflection



Shahzad/Zhu TUM/DLR-IMF



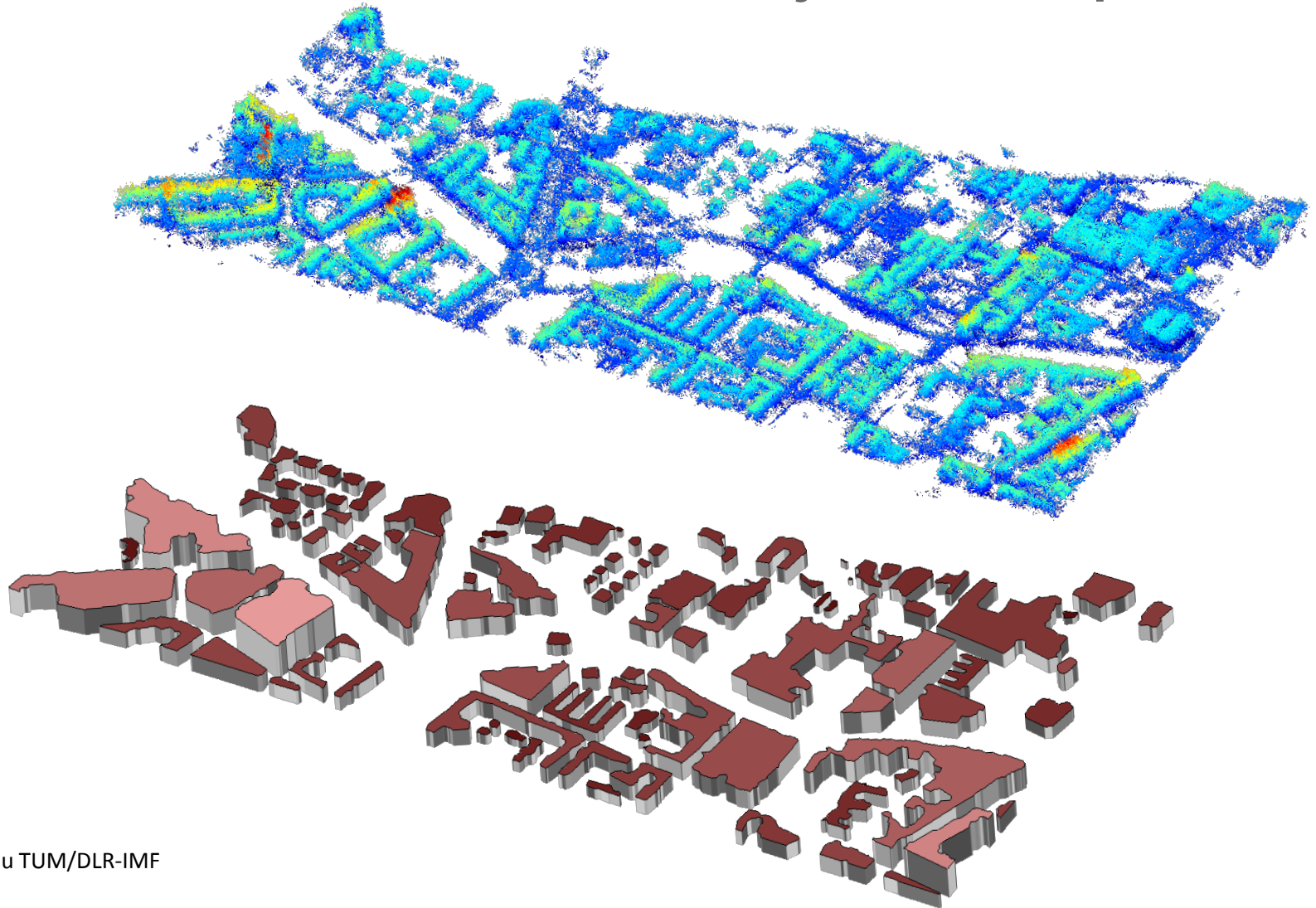
From TomoSAR Point Clouds to Objects – Façade



Shahzad/Zhu TUM/DLR-IMF



From TomoSAR Point Clouds to Objects – Footprint

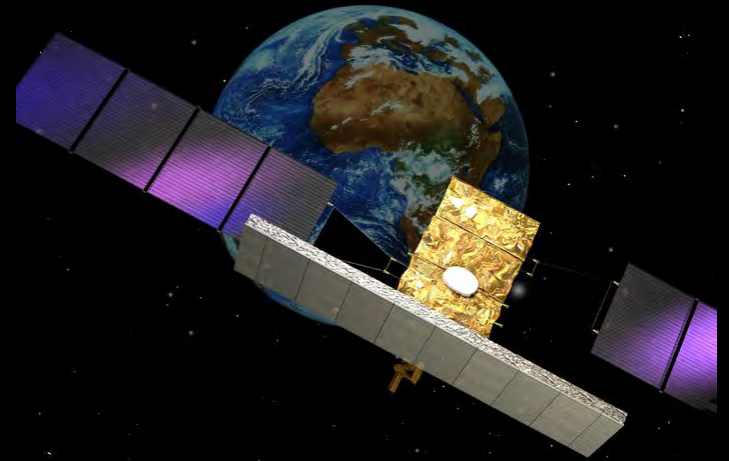


Shahzad/Zhu TUM/DLR-IMF





Sentinel-1A



Cosmo-SkyMed

What comes next?
MultiSensoral?



ALOS-2



TerraSAR-X/TanDEM-X